Cell Reports, Volume *40*

Supplemental information

Rhomboid protease RHBDL4 promotes retrotranslocation of aggregation-prone proteins for degradation

Josephine Bock, Nathalie Kühnle, Julia D. Knopf, Nina Landscheidt, Jin-Gu Lee, Yihong Ye, and Marius K. Lemberg

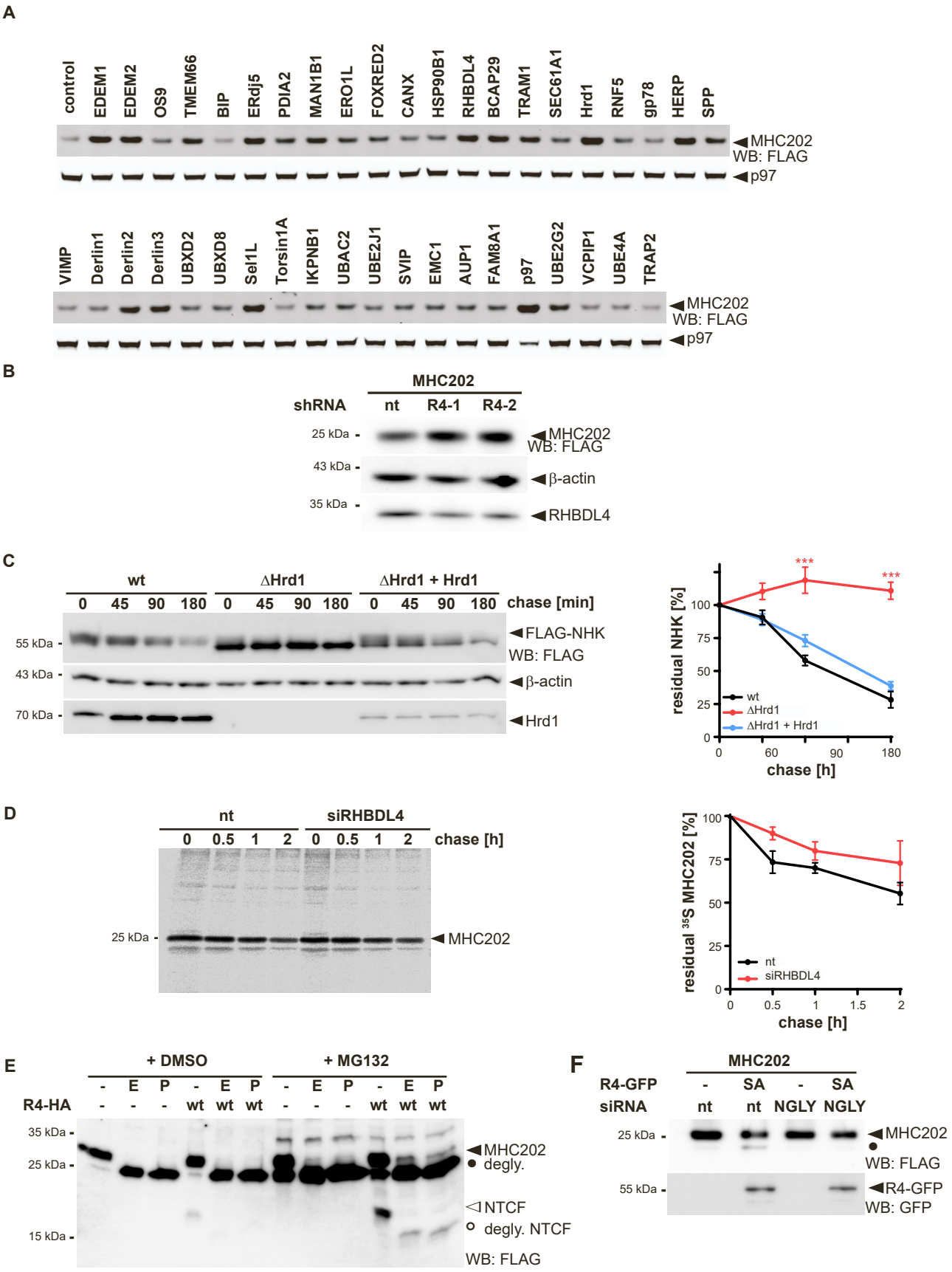

Figure S1. MHC202 is degraded by a concerted action of the Hrd1 complex and RHBDL4. Related to Figure 1.
(A) Influence of selected ERAD components on the steady-state level of MHC202 shown by western blot (WB) of lysates from siRNA transfected cells detecting the C-terminal FLAG tag. p97 was used as both positive and loading control. Knockdown efficiency of the siRNA screen was not determined and quantification of MHC202 steady-state level was not normalized to the loading control p97.
(B) RHBDL4 knockdown with two independent shRNAs (R4-1 and R4-2) in Hek293T cells leads to an increase of MHC202 steady-state level when compared to a non-targeting (nt) control shRNA. β-actin was used as a loading control.
(C) N-terminal FLAG-tagged NHK is stabilized in Hrd1 knockout cells (ΔHrd1) compared to parental Hek293T cells (wt). Co-expression of FLAG-NHK and Hrd1 rescues the degradation defect in ΔHrd1 cells. β-actin is used as a loading control. WB quantification of three independent experiments is shown in the right panel (means ± SEM, n=3, ***p ≤ 0.001 (two-way ANOVA)).

(D) siRNA knockdown of RHBDL4 delayed MHC202 degradation in Hek293T cells compared to the non-targeting siRNA control in metabolic pulse label chase. The right panel shows the quantification of autoradiograms of three independent experiments (means ± SEM, n=2).
(E) MHC202 (filled triangle) and its 18 kDa N-terminal fragment (NTCF) generated by ectopically expressed HA-tagged RHBDL4 (R4-HA) are glycosylated as shown by sensitivity to Endo H (E) and PNGase (P). Degly., deglycosylated full-length MHC202; Degly. NTCF , deglycosylated N-terminal cleavage fragment. Samples, as shown in Figure 1D, either treated with vehicle control (DMSO) or MG132 (2 μM).
(F) Stabilization of the unglycosylated form of MHC202 by the catalytic inactive mutant of RHBDL4 (SA-GFP) is abolished upon knockdown of N-glycanase (NGLY) when compared to nt control.
Data information: For clarity, for panels B-F representative experiments of three independent biological replicates are shown.

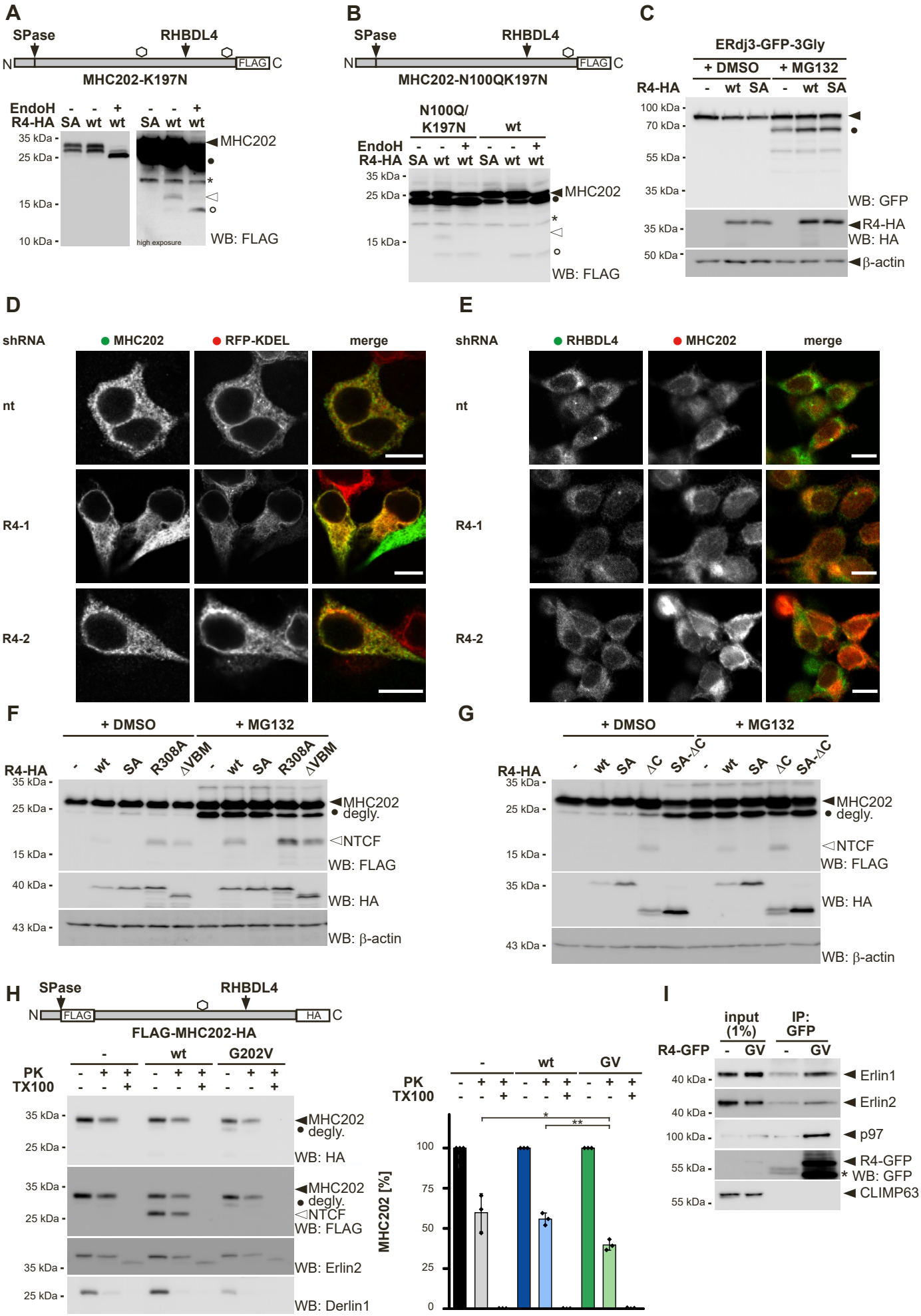
A
SPase
RHBDL4
N
FLAG
C
MHC202-K197N
EndoH
R4-HA
SA wt wt SA wt wt
35 kDa
25 kDa
15 kDa
10 kDa
MHC202
high exposure
WB: FLAG
B
SPase
RHBDL4
N
FLAG
C
MHC202-N100QK197N
N100Q/
K197N
wt
EndoH
R4-HA
SA wt wt SA wt wt
35 kDa
25 kDa
15 kDa
MHC202
WB: FLAG
C
ERdj3-GFP-3Gly
+ DMSO
+ MG132
R4-HA
- wt SA - wt SA
100 kDa
70 kDa
55 kDa
35 kDa
WB: GFP
R4-HA
WB: HA
50 kDa
β-actin
D
shRNA
MHC202
RFP-KDEL
merge
nt
R4-1
R4-2
E
shRNA
RHBDL4
MHC202
merge
nt
R4-1
R4-2
F
+ DMSO
+ MG132
R4-HA
- wt SA R308A ΔVBM - wt SA R308A ΔVBM
35 kDa
25 kDa
15 kDa
40 kDa
43 kDa
MHC202
degly.
NTCF
WB: FLAG
WB: HA
WB: β-actin
G
+ DMSO
+ MG132
R4-HA
- wt SA ΔC SA-ΔC - wt SA ΔC SA-ΔC
35 kDa
25 kDa
15 kDa
35 kDa
43 kDa
MHC202
degly.
NTCF
WB: FLAG
WB: HA
WB: β-actin
H
SPase
RHBDL4
N
FLAG
HA
C
FLAG-MHC202-HA
-
wt
G202V
PK
TX100
35 kDa
25 kDa
MHC202
degly.
WB: HA
MHC202
degly.
NTCF
WB: FLAG
35 kDa
WB: Erlin2
25 kDa
WB: Derlin1
-
wt
GV
PK
TX100
*
**
100
75
50
25
0
MHC202 [%]
I
input
(1%)
IP:
GFP
R4-GFP
- GV - GV
40 kDa
Erlin1
40 kDa
Erlin2
100 kDa
p97
55 kDa
R4-GFP
* WB: GFP
55 kDa
CLIMP63

Figure S2. RHBDL4 knockdown leads to accumulation of MHC202 in the ER. Related to Figure 2.
(A) RHBDL4 cleaves C-terminally FLAG-tagged MHC202 with an additional C-terminal glycosylation site (K197N) post-translocational as shown by the sensitivity of the C-terminal fragment to Endo H (open triangle and open circle).Asterix, unspecific band; filled circle, deglycosylated full-length MHC202; R4-HA, HA-tagged RHBDL4; hexagon, site for N-linked glycosylation; SPase, signal peptidase; WB, western blotting.
(B) RHBDL4 cleaves MHC202 lacking the native glycosylation site (N100Q) with a single glycosylation site (K197N) in the C-terminal portion leading to an Endo H-sensitive and a partially deglycosylated fragment (open triangle and open circle). Asterisk unspecific band; filled circle, deglycosylated full-length MHC202; hexagon, site of N-linked glycosylation; SPase, signal peptidase.
(C) RHBDL4 does not cleave ERdj3-GFP-3Gly (filled triangle). Deglycosylated ERdj3-GFP-3Gly (filled circle) is stabilized upon proteasomal inhibition by MG132 (2 μM). β-actin was used as a loading control.
(D) Knockdown of RHBDL4 with two independent shRNAs (R4-1, R4-2) leads to MHC202 accumulation in the ER as shown by colocalization with RFP-KDEL; nt, non-targeting control shRNA; scale bar, 10 μm.
(E) Knockdown of RHBDL4 with two independent shRNAs (R4-1, R4-2) increases MHC202 signal in stable T-REx Hek293T cell expressing FLAG-tagged MHC202, when compared to nt control shRNA; scale bar, 10 μm.
(F) The N-terminal cleavage fragment (NTCF) of C-terminally FLAG-tagged MHC202 generated by the HA-tagged RHBDL4-R308A mutant is stabilized in the absence of proteasome inhibitor MG132 (2 μM). Similarly, co-expression of an RHBDL4 mutant lacking the binding motif for p97 (ΔVBM) together with MHC202 results in stabilization of the N-terminal cleavage fragment. Impaired p97 interaction of RHBDL4 leads to a slightly reduced steady-state level of deglycosylated unprocessed MHC202 form (degly.). β-actin was used as a loading control.
(G) HA-tagged RHBDL4 mutant lacking the C-terminal domain (ΔC) cleaves FLAG-tagged MHC202 and stabilizes the deglycosylated unprocessed form of MHC202 even in the absence of proteasome inhibitor MG132 (2 μM). β-actin was used as a loading control.
(H) The accessibility of MHC202 to exogenous proteinase K (PK) was analyzed in ER-derived microsomes. Hek293T cells were co-transfected with double-tagged MHC202 and either an empty vector (-), RHBDL4 wt, or the RHBDL4-G202V mutant (G202V). Hek293T-derived microsomes were incubated with PK in the presence and absence of 1 % TritonX-100 (TX100). The R4-induced MHC202 cleavage fragment was protected from exogenous PK, whereas full-length MHC202 was partially accessible. Erlin2 (epitope in ER lumen) and Derlin1 (epitope in cytosol) were used as controls. Degly. , deglycosylated full-length MHC202. HA signals of three independent experiments were quantified and shown in the right panel (means ± SEM, n=3, *$p \leq 0.05$; **$p \leq 0.01$ (Student´s t-test)).
(I) GFP-tagged RHBDL4-G202V (R4GV-GFP) interacts with endogenous p97, Erlin1 and -2, but not CLIMP63 which was used as a negative control. Asterisk indicates unspecific band.
Data information: For clarity, for all panels representative experiments of three independent biological replicates are shown.

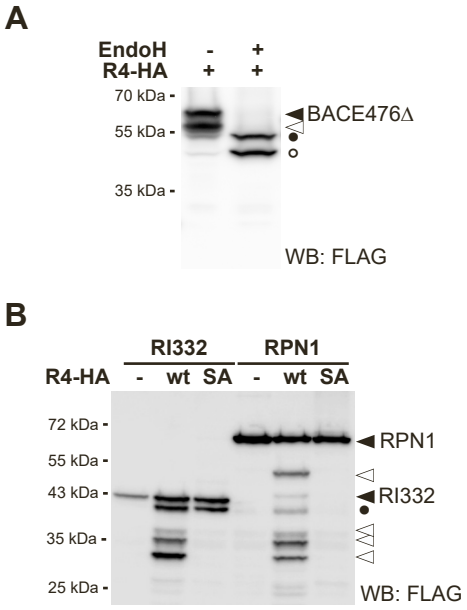

Figure S3. RHBDL4-catalyzed cleavage of BACE476Δ generates a glycosylated N-terminal fragment. Related to Figure 3.
(A) BACE476Δ (filled triangle) and its HA-tagged RHBDL4 (R4-HA) generated N-terminal fragment (open triangle) are glycosylated as shown by sensitivity to Endo H (filled and open circles). WB, western blotting.
(B) Hek293T cells were co-transfected either with RI332 or RPN1 and an empty vector (-), R4-HA wild type (wt), or the catalytic inactive SA mutant. RHBDL4 generates several N-terminal cleavage fragments (open triangles). Expression of the catalytic mutant stabilizes the 40-kDa deglycosylated full-length RI332 (filled circle) even in the absence of the proteasome inhibitor MG132 (2 μM).
Data information: For clarity, for all panels representative experiments of three independent biological replicates are shown.

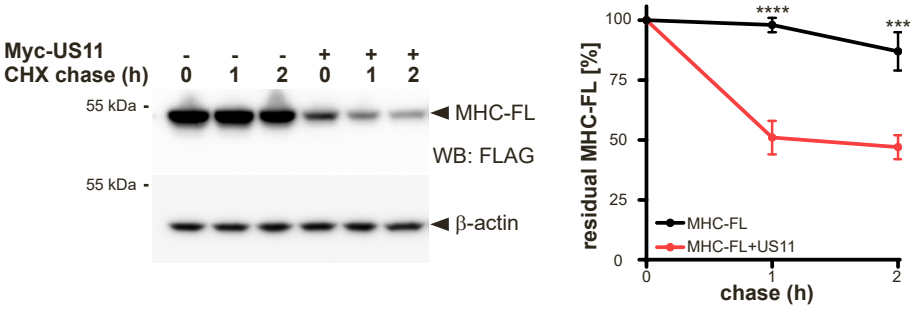

Figure S4. US11 increases turnover of MHC-FL. Related to Figure 4.
Hek293T cells were transfected with MHC-FL with or without Myc-tagged US11. 24 h post-transfection cycloheximide (CHX) was added, and cells were harvested at indicated time points (means ± SEM, n=4;***p ≤ 0.001, ****p ≤ 0.0001 (two-way ANOVA)). A representative experiment of three independent biological replicates is shown. WB, western blotting.

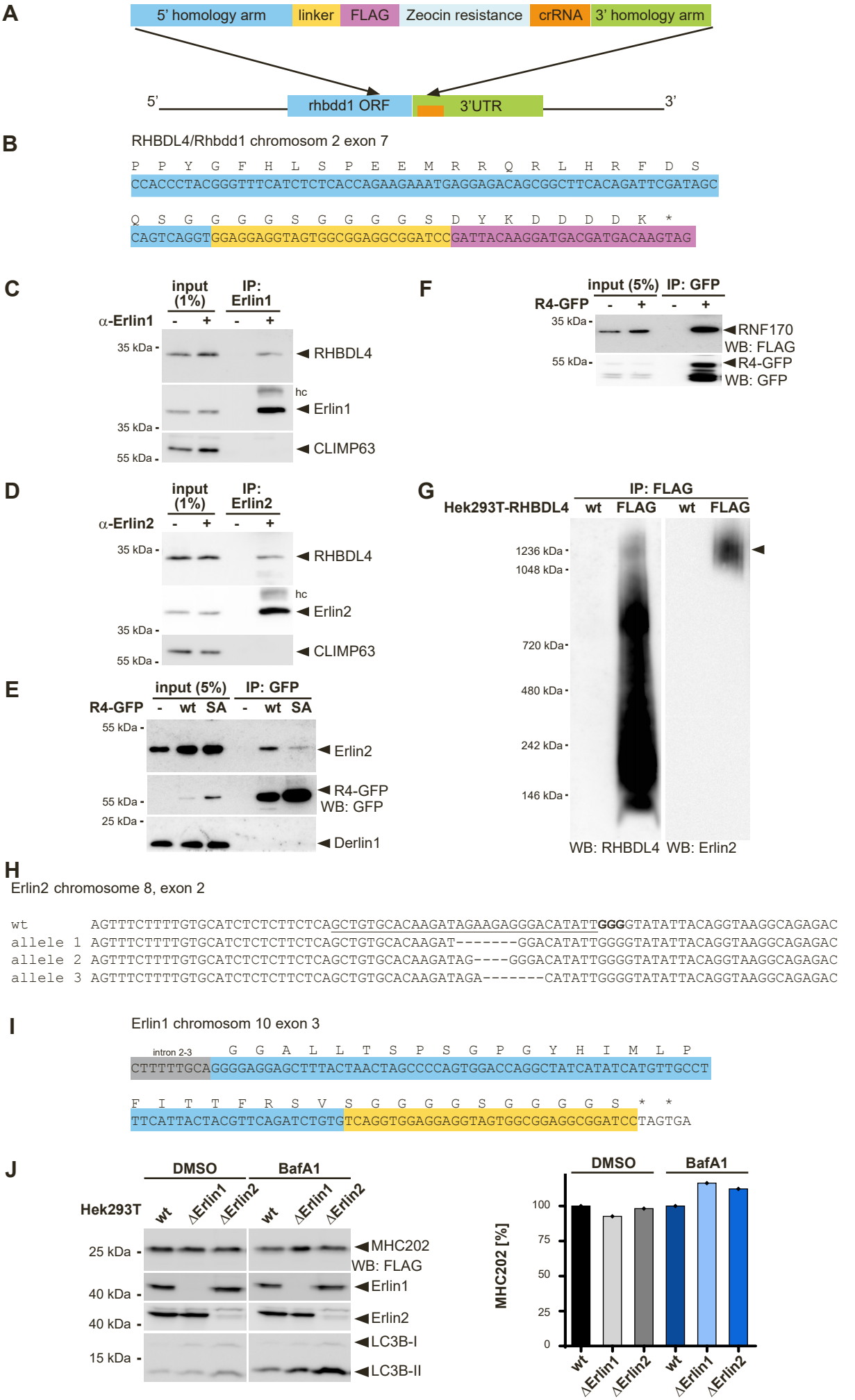
A
5' homology arm
linker
FLAG
Zeocin resistance
crRNA
3' homology arm
5'
rhbdd1 ORF
3'UTR
3'
B
RHBDL4/Rhbdd1 chromosom 2 exon 7
P P Y G F H L S P E E M R R Q R L H R F D S
CCACCCTACGGGTTTCATCTCTCACCAGAAGAAATGAGGAGACAGCGGCTTCACAGATTCGATAGC
Q S G G G G S G G G G S D Y K D D D D K *
CAGTCAGGTGGAGGAGGTAGTGGCGGAGGCGGATCCGATTACAAGGATGACGATGACAAGTAG
C
input (1%)
IP: Erlin1
α-Erlin1
35 kDa
RHBDL4
hc
Erlin1
35 kDa
55 kDa
CLIMP63
D
input (1%)
IP: Erlin2
α-Erlin2
35 kDa
RHBDL4
hc
Erlin2
35 kDa
55 kDa
CLIMP63
E
input (5%)
IP: GFP
R4-GFP
wt
SA
55 kDa
Erlin2
55 kDa
R4-GFP
WB: GFP
25 kDa
Derlin1
F
input (5%)
IP: GFP
R4-GFP
35 kDa
RNF170
WB: FLAG
55 kDa
R4-GFP
WB: GFP
G
IP: FLAG
Hek293T-RHBDL4
wt
FLAG
1236 kDa
1048 kDa
720 kDa
480 kDa
242 kDa
146 kDa
WB: RHBDL4
WB: Erlin2
H
Erlin2 chromosome 8, exon 2
wt AGTTTCTTTTGTGCATCTCTCTTCTCAGCTGTGCACAAGATAGAAGAGGGACATATTGGGGTATATTACAGGTAAGGCAGAGAC
allele 1 AGTTTCTTTTGTGCATCTCTCTTCTCAGCTGTGCACAAGAT-------GGACATATTGGGGTATATTACAGGTAAGGCAGAGAC
allele 2 AGTTTCTTTTGTGCATCTCTCTTCTCAGCTGTGCACAAGATAG----GGGACATATTGGGGTATATTACAGGTAAGGCAGAGAC
allele 3 AGTTTCTTTTGTGCATCTCTCTTCTCAGCTGTGCACAAGATAGA-------CATATTGGGGTATATTACAGGTAAGGCAGAGAC
I
Erlin1 chromosom 10 exon 3
intron 2-3
G G A L L T S P S G P G Y H I M L P
CTTTTTGCAGGGGAGGAGCTTTACTAACTAGCCCCAGTGGACCAGGCTATCATATCATGTTGCCT
F I T T F R S V S G G G G G S G G G G S * *
TTCATTACTACGTTCAGATCTGTGTCAGGTGGAGGAGGTAGTGGCGGAGGCGGATCCTAGTGA
J
DMSO
BafA1
Hek293T
wt
ΔErlin1
ΔErlin2
25 kDa
MHC202
WB: FLAG
40 kDa
Erlin1
40 kDa
Erlin2
LC3B-I
15 kDa
LC3B-II
MHC202 [%]
100
75
50
25
0

Figure S5. RHBDL4 interacts with Erlin1, Erlin2 and RNF170. Related to Figure 5.
(A) Outline of the applied tagging strategy of RHBDL4 (referred to by its gene name Rhbdd1) according to (Fueller et al., 2020).
(B) Sanger sequencing of chromosomal DNA obtained from the Hek293T-R4-FLAG cell lines shows the insertion of the FLAG tag in the last coding exon. Color code as in (A).
(C) Microsomes from Hek293T cells were solubilized with 1% Triton X-100, and endogenous Erlin1 was isolated by immunoprecipitation (IP). Western blot (WB) identifies co-purification of endogenous RHBDL4. Hc, heavy chain.
(D) Microsomes from Hek293T cells were solubilized with 1% Triton X-100, and endogenous Erlin2 was isolated by IP. WB identifies co-purification of endogenous RHBDL4. Hc, heavy chain.
(E) Hek293T cells were transfected with empty vector, RHBDL4-GFP or catalytic inactive RHBDL4-SA-GFP (SA). Following solubilization with Triton X-100, R4-GFP was isolated by IP using an anti-GFP antibody. Endogenous Erlin2 binds more efficiently to R4-GFP wild type (wt) than to its catalytic inactive SA mutant. Derlin1 was used as a negative control.
(F) Co-immunoprecipitation experiment as in (C) using Hek293T cells transfected with RNF170-FLAG.
(G) Endogenous RHBDL4 is part of an MDa-sized erlin complex. Hek293T wt cells or cells with chromosomally FLAG-tagged RHBDL4 (FLAG) were solubilized with 1% Triton X-100, immunoprecipitated for FLAG, eluted with FLAG peptides and analyzed by BN-PAGE. RHBDL4-FLAG formed several higher molecular weight complexes in addition to the 1.2 MDa complex containing Erlin2 (filled triangle).
(H) Sanger sequencing of genomic DNA obtained from Hek293T ΔErlin2 knockout cells. Single-guide RNA-binding site is underlined; protospacer-associated motif is shown in bold.
(I) Sanger sequencing of genomic DNA obtained from Hek293TΔErlin1 knockout cells show the insertion of the Stop cassette in exon 3. Color code as in (A). Erlin1/Erlin2 double knockout cells were generated accordingly using the Erlin2 knockout cells in (H).
(J) Steady-state levels of MHC202 are reduced in Hek293T Erlin1 (ΔErlin1) and Erlin2 (ΔErlin2) knockout cells compared to wt Hek293T cells. Lysosomal inhibition by BafA1 increases stabilization of MHC202 caused by single knockout of Erlin1 and Erlin2 (n=1).

Data information: For clarity, for panels C-G representative experiments of three independent biological replicates are shown.

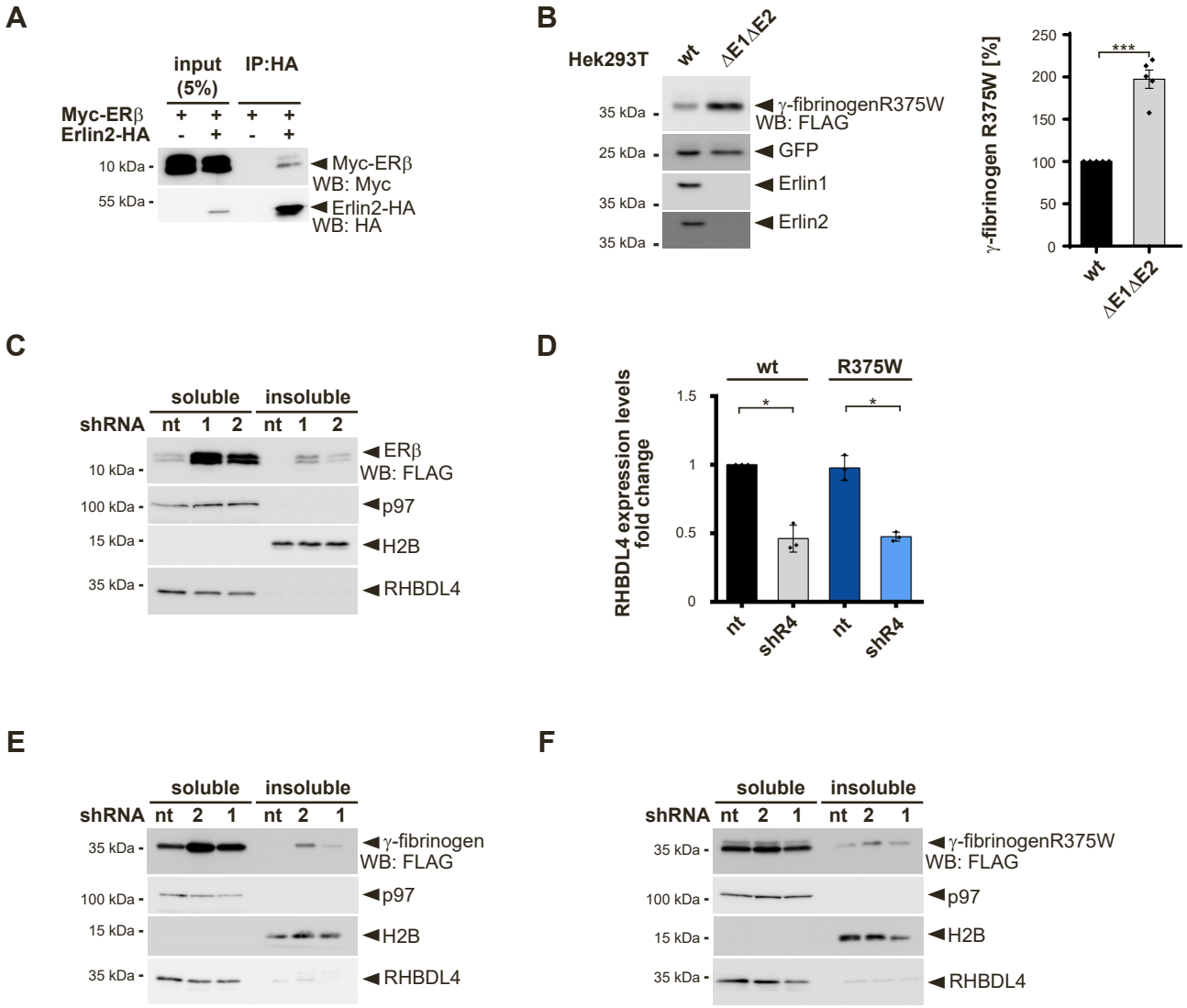

Figure S6. The RHBDL4-erlin complex interacts with aggregation-prone proteins. Related to Figure 6.
(A) Western blotting (WB) after immunoprecipitation (IP) of Erlin2-HA from Triton X-100 solubilized Hek293T cells confirms interaction with ERβ as has been shown previously (Vincenz-Donnelly et al., 2018).
(B) Steady-state levels of γ-fibrinogen R375W mutant increase in Erlin1/Erlin2 Hek293T double knockout cells (ΔE1ΔE2) in comparison to parental wild-type Hek293T cells (wt). GFP was used as a loading control. Right panel, WB quantification of γ-fibrinogen R375W (means ± SEM, n=5, ***p≤ 0.001 (Student´s t-test)).
(C) ERβ steady-state levels increase in Hek293T cells transfected with two independent shRNAs targeting RHBDL4 (R4-1 and R4-2) compared to non-targeting control (nt). Knockdown of RHBDL4 further increases the recovery of ERβ in the NP40 insoluble fraction. p97 was used as a loading control for the soluble fraction and H2B for the insoluble fraction.
(D) Transcriptional levels of RHBDL4 are reduced upon knockdown of RHBDL4 (shR4) compared to cells co-transfected with nt control and γ-fibrinogen wt or R375W mutant. (means ± SEM, n=3, *p≤ 0.05, **p≤ 0.01 (Student´s t-test)).
(E) γ-fibrinogen steady-state levels increase in Hek293T cells transfected with two independent shRNAs targeting RHBDL4 (R4-1 and R4-2) compared to cell treated with nt control in Hek293T cells. Knockdown of RHBDL4 further increases the recovery of γ-fibrinogen in the NP40 insoluble fraction. p97 was used as a loading control for the soluble fraction and H2B for the insoluble fraction.
(F) Assay as shown in (E) analyzing the steady-state levels of the γ-fibrinogen R375W mutant. Knockdown of RHBDL4 further increases the recovery of γ-fibrinogen R375W in the NP40 insoluble fraction. p97 was used as a loading control for soluble fraction and H2B for insoluble fraction, respectively.
Data information: For clarity, for panels A and C-F representative experiments of three independent biological replicates are shown. For panel B a representative experiment of five independent biological replicates is shown.

target gene	sequence
Erlin1-fwd	5'-CCAGAGGTACGGTTGGTTGA-3'
Erlin1-rev	5'-CCTTCCAAGCTTCCTGGTTCA-3'
Erlin2-fwd	5'- CTTGAGCAACGGCTGTATCC-3'
Erlin2-rev	5'- AATCACCACCCATGGCATCAT-3'
Hrd1-fwd	5' GGCTATTTTGCACAGCACGA-3'
Hrd1-rev	5'-CTTCCACCTGCTCCAGAACT-3'
RHBDL4/RHBDD1-fwd	5'-TTATGGAGCACGATGGAAGGAA-3'
RHBDL4/RHBDD1-rev	5'-GAGATGGGAGCGTGGAAACT-3'

Table S3. Primers used for validation of the generated cell lines. Related to the STAR Methods.

target gene	sequence
BiP	5'-CCAACGCCAAGCAACCAAAG-3' 5'-TGCCGTAGGCTCGTTGATG-3'
β-2 microglobulin	5'-CACGTCATCCAGCAGAGAAT-3' 5'-TGCTGCTTACATGTCTCGAT-3'
RHBDL4/RHBDD1	5'-GGTCGTAGAGAGCGTTCAGC-3' 5'-CTTGATCTCCGTTGCATGGC-3'
TATA-binding protein	5'-CCGGCTGTTTAACTTCGCTT-3' 5'-ACGCCAAGAAACAGTGATGC-3'
XBP1	5'-CCTGGTTGCTGAAGAGGAG-3' 5'-CCATGGGGAGATGTTCTGG-3'

Table S4. Primers used for cDNA synthesis. Related to the STAR Methods.

plasmid	Source
BACE476Δ	gift from M. Molinari
γ-fibrinogen wt	gift from J. Brodsky
γ-fibrinogen-R375W	gift from J. Brodsky
ERdj3-GFP-3Gly	gift from M. Schuldinger
FLAG-Erlin1	gift from R. Wojcikiewicz, Pearce et al., 2007;
FLAG-Erlin2	gift from R. Wojcikiewicz, Pearce et al., 2007;
FLAG-RNF170	gift from R. Wojcikiewicz, Pearce et al., 2008
3FLAG-γ-fibrinogen wt	This paper
3FLAG-γ-fibrinogen-R375W	This paper
3-FLAG-MHC-FL	This paper
3FLAG-MHC121	This paper
3FLAG-MHC202	This paper
3FLAG-MHC202-3HA	This paper
3FLAG-MHC202_IRES_GFP	This paper
3FLAG-MHC202-K197N	This paper
3FLAG-MHC202-N100Q-K197N	This paper
3FLAG-MHC202-PP	This paper
3FLAG-MHC202-pTα	This paper
3FLAG-NHK	This paper
3FLAG-OS9	This paper
3FLAG-RI332	Fleig et al., 2012
3HA-Erlin2	This study
3HA-RHBDL4	This paper
3HA-RHBDL4-ΔC	Fleig et al., 2012
3HA-RHBDL4-SA-ΔC	Fleig et al., 2012
3HA-RHBDL4-ΔVBM	Fleig et al., 2012
3HA-RHBDL4-G198V	This paper
3HA-RHBDL4-G202V	This paper
3HA-RHBDL4-SA	Fleig et al., 2012

Hrd1 ORF	gift from E. Krüger, Steffen et al., 2010
NHK ORF	gift from R. Kopito
Myc-Erbeta	gift from M. Hipp
Myc-Erbeta-3FLAG	This paper
Prolactin	Fleig et al., 2012
Prolactin-KDEL	Fleig et al., 2012
RFP-KDEL	Altan-Bonnet et al., 2006
RHBDL4-FLAG	This paper
RHBDL4-GFP	Fleig et al., 2012
RHBDL4-SA-GFP	Fleig et al., 2012
RHBDL4-G202V-GFP	This paper

Table S5. Plasmids used in this paper. Related to the STAR Methods.